



*LIGO Laboratory / LIGO Scientific Collaboration*

LIGO-T000127-v4

*ADVANCED LIGO*

3/10/2015

---

Core Optics Components  
Design Requirements Document

---

G. Billingsley, G. Harry, W. Kells

Distribution of this document:  
LIGO Science Collaboration

This is an internal working note  
of the LIGO Project.

**California Institute of Technology**  
LIGO Project – MS 18-34  
1200 E. California Blvd.  
Pasadena, CA 91125  
Phone (626) 395-2129  
Fax (626) 304-9834  
E-mail: [info@ligo.caltech.edu](mailto:info@ligo.caltech.edu)

**Massachusetts Institute of Technology**  
LIGO Project – MIT NW22-295  
185 Albany St  
Cambridge, MA 02139  
Phone (617) 253-4824  
Fax (617) 253-7014  
E-mail: [info@ligo.mit.edu](mailto:info@ligo.mit.edu)

**LIGO Hanford Observatory**  
P.O. Box 1970  
Mail Stop S9-02  
Richland WA 99352  
Phone 509-372-8106  
Fax 509-372-8137

**LIGO Livingston Observatory**  
P.O. Box 940  
Livingston, LA 70754  
Phone 225-686-3100  
Fax 225-686-7189

<http://www.ligo.caltech.edu/>

**Table of Contents**

<b>1</b>	<b>Introduction</b>	<b>4</b>
1.1	Purpose	4
<b>2</b>	<b>Scope</b>	<b>5</b>
2.1	Definitions	5
2.2	Acronyms	5
2.3	Applicable Documents	6
2.3.1	LIGO Documents	6
2.3.2	Non-LIGO Documents	8
<b>3</b>	<b>General description</b>	<b>9</b>
3.1	Product Functions	9
3.1.1	Product layout	10
3.2	General Constraints	10
3.2.1	Simplicity	10
3.2.2	Basic Shape	11
3.2.3	Continuous operation	11
3.2.4	Substrate material	11
3.3	Assumptions and Dependencies for this document	11
<b>4</b>	<b>Requirements</b>	<b>13</b>
4.1	Introduction	13
4.2	Characteristics	14
4.2.1	Performance Characteristics	14
4.2.2	Physical Characteristics	15
4.2.3	Interface Definitions	32
4.2.4	Reliability	33
4.2.5	Maintainability	34
4.2.6	Environmental Conditions	34
4.2.7	Transportability	35
4.3	Design and Construction	36
4.3.1	Materials and Processes	36
4.3.2	Workmanship	37
4.3.3	Interchangeability	37
4.3.4	Safety	37
4.3.5	Human Engineering	37

**Table of Tables**

<i>Table 1 Performance requirement flow down</i>	<u>13</u>
<i>Table 2 Physical Parameters of Interferometer COC</i>	<u>16</u>
<i>Table 3 Optical Parameters of the PRC and SRC</i>	<u>22</u>
<i>Table 4 Required Limits on Sources of Wave-front Distortion (surface 1)</i>	<u>26</u>
<i>Table 5 Specified Limits to Losses (in ppm) in COC</i>	<u>31</u>
<i>Table 6 Environmental Performance Characteristics</i>	<u>35</u>

# 1 Introduction

## 1.1 Purpose

This Design Requirements Document (DRD) for the Core Optics Components (COC) subsystem identifies the information necessary to define the COC subsystem and quantify its relationship to other LIGO subsystems. Requirements, formally flowing down from the Systems (SYS) task, are stated to provide a full description of the COC and their optical and physical properties. As of this draft, COC will limit interferometer performance at the detector's most sensitive range due to thermal noise in the coatings. Models indicate that COC will also limit detector sensitivity at high frequency due to power lost in the arm cavities by imperfect optics. As such, it is the goal of COC to provide the best optics obtainable within reasonable fiscal constraints.

## 2 Scope

This document will detail requirements on the 13 “Core” optical elements (COC) necessary for each Advanced LIGO interferometer. Reference to other subsystems will be made only to define interfaces, clarify rationale for requirements, and provide justification of required parameters. Note that any metrology equipment or procedures adopted by Advanced LIGO for verification of the specifications and requirements herein are treated separately (LIGO-

The original development plan for manufacture and test of the optics was the COC development plan, LIGO-T000128. The design that specifically meets the requirements of this document and is the baseline for the Advanced LIGO COC is described in the COC Preliminary Design LIGO-E080033-00-D. This version of Advanced LIGO COC DRD (LIGO-T000127-v3) represents a revision of the earlier (7/2010) version (LIGO-T000127-v2) presented as FDR documentation.

### 2.1 Definitions

#### 2.1.1.1 Physical Definitions

Physically, the COC subsystem consists of the following items:

**Distinct optical elements:**

- Test Masses (TM) of two types: Input TM (ITM) and End TM (ETM).
- Beamsplitter (BS).
- Power Recycling Mirror (PRM).
- Signal Recycling Mirror (SRM)
- Power and Signal Recycling Telescope (PR/SR 2,3) optical elements.
- Compensation Plates (CP), one for each ITM

**Coatings to be applied to these elements:**

- Anti reflectance coating applied to surface 2 of each optic and to both surfaces of the compensation plate.
- High reflectance coating applied to surface 1 of each optic.
- Gold ESD coating on the Compensation plate surface 1 (surface facing ITM surface 2).

### 2.2 Acronyms

- Throughout this document items will be mentioned whose existence, scope, or value are yet to be determined. A symbol <sup>TBD</sup> represents this status.
- IFO= Interferometer
- ASC= Alignment sensing and control subsystem.

- AOS= Auxiliary Optics System. A critical subsystem of this is the TCS= Thermal Compensation System, which maintains the correct COC optical properties under high beam power thermal loading.
- CD= Contrast defect:  $CD_c$  for carrier power;  $CD_{sb}$  for side band power.
- ESD= electro-static drive (referring to actuation method for test masses).
- FFT model: the standard computer simulation of the static LIGO IFO
- GW= gravitational wave.
- L and  $L_A$  will mean length and arm cavity length respectively.
- G= Power recycling cavity gain:  $G_c$  for carrier power;  $G_{sb}$  for side band power.
- HR= high reflectivity (refers to the primary beam manipulating surface of any COC)
- HTM= higher transverse modes.
- IOO= Input/Output optics.
- "in-line" and "out-line": refer to the two IFO arms. The in-line arm is the one whose beam has transmitted through the BS.
- $\lambda_s$  = optical surface spatial wavelength.
- OPD= optical path difference, a standard optics metrology term
- PF = pathfinder (program of full sized trial TMs sent through full polish processing at prospective vendors)
- Power loss to any specified beam mode is designated  $\mathcal{L}$  (e.g.  $\mathcal{L}_A$  for arm cavity RT loss)
- $\phi$ ,  $h$ , = diameter, thickness of optics.  $\phi_s$ ,  $h_s$  would specify substrate diameter and thickness.
- $R_{eff}$ = the effective radius of curvature (ROC) for a mirror surface as seen by an incident Gaussian beam.
- $\Delta R_{rep}$  = the tolerance on fabrication reproducibility of nominally identical spherical reflecting surfaces (includes substrate figuring and added coatings)
- SUS= Suspension design system.
- SYS= Detector Systems Engineering/Integration.
- $w_0$  = Primary cavity's beam Gaussian waist radius.  $w_{xx}$  indicates beam Gaussian radius at location xx. For example  $w_{ETM}$  will be the end test mass beam radius.
- YAG= 1.064 micron laser or laser light (wavelength  $\lambda$  if not otherwise specified).

## 2.3 Applicable Documents

### 2.3.1 LIGO Documents

Core Optics Components Preliminary Design Document: LIGO-E080033

Advanced LIGO Coating Program and Specification: LIGO-E000487

Advanced LIGO Coating Development Plan: LIGO-C030187-00-R  
*LASTI Test Mass Coating Characterization*, LIGO-T070233  
*LASTI Test Mass Handling and Shipping Procedures*, LIGO-T070070  
COC Subsystem Development Plan: LIGO-T000128  
*Test Mass Material Down-Select Plan*, LIGO-T020103-04  
*Advanced LIGO Substrate Selection Recommendation*, LIGO-M040405-00  
Dimensions for Advanced LIGO Fused Silica Test Masses, LIGO-T040199-00  
Advanced LIGO Systems Design LIGO-T010075-v3  
AdvLIGO Interferometer Sensing and Control Conceptual Design, LIGO-T070247-01  
Thermal Compensation Update, LIGO-G020502-00-R and MIT thesis, R. Lawrence, 2003.  
Thermal Noise in Interferometric Gravitational Wave Detectors Due to Dielectric Optical Coatings:  
LIGO-P020005-00-Z  
*Dimensions for Advanced LIGO FS Test Masses*, LIGO-T040199-00-R.  
LIGO-E030647-01-D  
*TM Thermal Compensation Strategies*, LIGO-T060214-01.  
*Transmission Requirements for ETM and ERM*, LIGO-M080042  
IOO PDR document: LIGO-T060269-02-D  
Note on RC matching..... LIGO-T080198-00  
Basic (“ABCD”) distortion through a prism (wedge effect) described in LIGO-T070039, Sect. 9.1.3  
*Design of the Advanced LIGO Recycling Cavities*, LIGO-P080004-00-Z (Optics Express **16**, 10018)  
Input Output Procurement Readiness, LIGO-T080075-01-D  
*Optical Layout and Parameters for the Advanced LIGO Cavities*, LIGO-T0900043-v11  
*Arm Cavity Finesse for Advanced LIGO*, LIGO-T070303-01-D  
AOS-TCS conceptual designs, LIGO-T060083-01-D  
*Beamsplitter First Elastic Mode Frequency versus Dimensions*, LIGO-T040232-00  
*Scattering Light Loss from LIGO Arm Cavity Mirrors*, LIGO-T0900128-v3  
*Analysis of scattering loss in AdvLIGO arm*, [LIGO-T0900159-v1](#)  
*Modal Diffraction Loss*, LIGO-T080392-v1  
*Astigmatism by the stable Michelson cavity*, LIGO-T0900384-v1  
*Effects of small size anomalies in a FP cavity*, LIGO-T1000154-v5  
*Mode matching and diffraction loss of FP cavity with thermal deformations*, LIGO-T0900306-v6  
*Advanced LIGO Baffle Design Using SIS*, LIGO-T1000090-v3

Many requirements are developed from earlier, generic studies:

LIGO I Science Requirements Document: LIGO-E950018-00-E

Advanced LIGO COC sizes decisions : LIGO-M050397-02, M070420-02, M040006, M040005, M060305-01.

Optical Wave front Distortion Specification notes (R. Weiss) LIGO-T952009-00-E

Electrostatic Charging on TMs (FJR) L960044-00-E

COC cleaning protocols in LIGO-E990035-C, LIGO-E070304-00, LIGO-E070292.

AR/ER coating properties (H. Yamamoto) LIGO-G950043

FFT model description (B. Bochner, Y. Hefetz) LIGO-G950061-01-R and Thesis, B. Bochner, MIT, 2000.

### **2.3.2 Non-LIGO Documents**

VIRGO Final Design (report) Ver. 0. June 1995

Thesis, P. Hello. University of Paris, 1994.

W. Winkler, et. al., Optics Comm., 112, 245(1994).

W. Winkler, et. al., Phys. Rev. A44, 7022

### 3 General description

#### Product Perspective

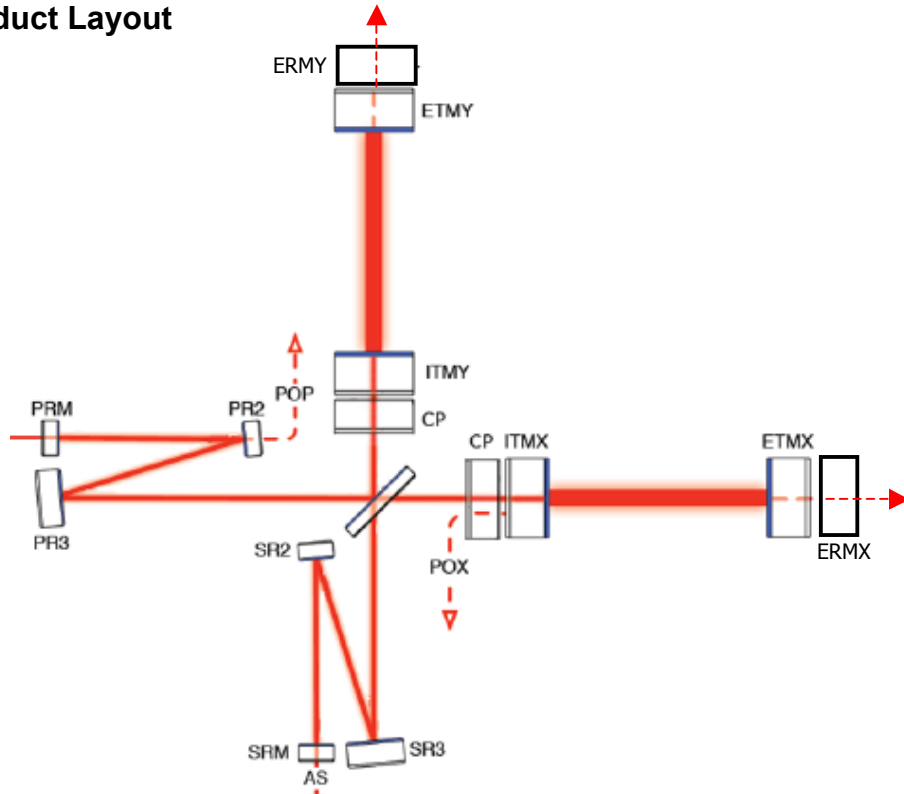
The Core Optics Components (COC) provide an “optical plant configuration” of stable, low loss optical cavities to be implemented for the optimal detection of gravitational waves within the LIGO design bandwidth. Thus the COC interfaces optically with the Input Optics (IO) and ASC subsystems. COC are aligned via optical interface and thermal control, with sensing systems provided by Auxiliary Optics System (AOS). The only mechanical interface is to Suspensions (SUS) (specified by the SUS DRD) via contacting suspension elements.

#### 3.1 Product Functions

The main functions of the COC are:

- Provide a high performance  $TEM_{00}$  (optimally matched to the IO beam  $TEM_{00}$  mode) mode optical cavity interferometer, which is maximally sensitive to gravitational waves.
- Provide appropriate beam pick-off points, allowing routing of samples of the optical cavity light to various gravitational wave, length and alignment sensing detectors.
- Minimize stray/scattered light from the optical cavities and surfaces.
- Minimize thermal mode noise from the body and face of the optic and the interfacing suspension components.
- Optimize the overall optical configuration to minimize the effects of optical distortions due to beam heating at full power operation.
- Provide an initial [cold] optical configuration whose lens powers; thermal properties; and tolerances are compatible with the dynamic range of the TCS.

### 3.1.1 Product Layout



Schematic layout of the COC elements for the non-folded interferometers. The folded interferometer includes, in addition,  $45^\circ$  incident nominally plane FM beam turning mirrors placed in the path between the BS and CP elements above. The ERM are part of the SUS subsystem.

## 3.2 General Constraints

Realistic feasibility constraints have guided the nature of the requirements from the outset of the Advanced LIGO program. We mention the main ones here:

### 3.2.1 Simplicity

The basic GW IFO configuration, specified by SYS, should be simple in terms of COC number and type:

- Each optic contributes additional wave front distortion, which degrades performance.
- Each COC optic necessitates an additional control servo and suspension system, which degrades performance.
- Contamination potential is proportionally reduced.
- Overall system design is significantly eased, clear optical lines of sight are increased.
- Physically similar COC simplify optical fabrication, IFO construction, spares inventory, handling fixtures and testing.

This document assumes a minimal IFO component count of two optics constituting each arm cavity; and nine optics constituting the recycling cavities.

### 3.2.2 Basic Shape

The COC are to be fabricated within the constraints of the ultra high precision optical industry. This framework virtually determines the choice of substrate geometrical shape (circular cylinder, possibly with wedged faces). Additional reasons for this shape include:

- The natural shape for the COC optical faces is circular, matching the TEM<sub>00</sub> mode symmetry.
- Understanding of the internal mechanical mode spectrum and influence is simplified by this choice.

We therefore assume without further detailed discussion that the all COC are of the basic right circular cylinder shape.

### 3.2.3 Continuous operation

LIGO must operate with high availability; therefore the COC must be designed with high reliability and low mean time to repair. Spares will be prepared to provide required availability, since the fabrication of precision optics is a lengthy process.

### 3.2.4 Substrate material

Fused Silica (FS) is chosen as the COC test mass material baseline. This decision was made in December of 2004 and is documented in M040405-00-R.

Fused silica is also the material for all other COC [recycling cavity] elements due to the body of optical industry and LIGO experience with this material. Different quality grades of fused silica are to be specified for the various COC elements to optimize their required performance.

## 3.3 Assumptions and Dependencies for this document

- The primary laser beam light is at 1064 nm (YAG).
- A stable, curved-curved arm cavity configuration with cavity length = 3994.75 m is assumed.
- The two IFO arm cavities are oriented in the same plane at 90°. This requires a 45° oriented BS element. This BS is assumed to split the two arm beams at the coating on its surface (surface 1) which faces the Power Recycling mirror. The polarization of the LIGO laser beam is in the plane defined by the interferometer arm axes, “P” polarization wrt the BS (~ in the plane of the ground surface).
- The primary optical HR and AR coatings on the COC substrates will be multilayer, dielectric thin films applied by Ion beam deposition

- Recycling cavity optics (PRM, SRM, BS, CP) will be suspended by wire loop type design . All Test Masses will be suspended by attachment of FS ribbons or fibers (SUS design).
- All COC are of the right circular cylinder form with slight departure for interface to other subsystems, for instance AR surfaces at small wedge angles with respect to the normal to the interferometer plane.
- All COC optical surfaces are to have nominally flat surfaces except for the primary (HR) ETM, ITM, PRM ,SRM, and P/SRM Telescope surfaces which are assumed to be sections of spheres with the effective radii of curvature adjusted to maintain a stable, single consistent Gaussian mode.
- For purposes of this document the Recycling cavities (PRC and SRC) are required to be stable designs (of a type described in LIGO-P080004-00-Z). Physically this entails a six element PRC/SRC design such that a two element (all reflective) “telescope” expands the input beam, small waist radius ( $\sim 2\text{mm}$ ) at the RM to full arm cavity size ( $\sim 55\text{mm}$ ) at the ITM. In this case the RM is physically a small optic, and at least one telescope optic is approximately full TM size.
- A tentative “low finesse” arm cavity design is taken (unless otherwise considered). Quantitatively this means arm cavities with optical finesse  $\sim 450$ . This is significantly lower than called for in the reference design ( LIGO-T010075-00) and reflects revisions argued in LIGO-T070247-00-I and LIGO-T070303, culminating in LIGO-T010075-01-I).

## 4 Requirements

### 4.1 Introduction

Primarily the COC requirements flow down from those determined by SYS to be appropriate for the Advanced LIGO. Of secondary consideration are requirements for engineering of other subsystem components. For instance the specification of wedge angles for the TM surface 2 to facilitate implementation of the sensing systems is strictly subordinate to this specification and should not negatively impact the TM optical cavity performance. Table 1 summarizes such flow down from primary requirements of the detector (or subsystems) to requirements of COC and other subsystems.

**Table 1 Performance requirement flow down**

Requirement on COC	Other Subsystem	Other Subsystem Requirement Category	Primary Requirement Mechanism
Number of pick-off surfaces for length control	SYS	IFO configuration	Necessity of inter cavity signal for orientation & length control
Substrate bulk optical quality	SYS	IFO Cavity Power gains	Minimize loss to bulk scattering mechanisms
Element optical surface quality			Minimize loss to surface scatter out of TEM <sub>00</sub>
Substrate bulk optical quality	SYS	Dark port contrast defect.	Wave front distortion: bulk inhomogeneities
Element optical surface quality		Mode matching between cavities and beam from IO	Wave front distortion: surface irregularities
Coating absorption	SYS	Arm cavity intensity limitation.	Minimize thermal distortion of elements.
	AOS/TCS	Compensation	
Mean TM R <sub>eff</sub>	SYS	IFO TEM <sub>00</sub> mode size	Optimize arm mode edge diffractive loss vs HR thermo-elastic noise.
Element mass and aspect ratio	SYS	Circulating cavity power	Balance radiation pressure
		Scattering loss to baffles.	Optimum substrate Diameter
		Thermal noise	Optimum effective optical Diameter see T040199-00

Surface reflectivity at wavelengths other than carrier	AOS (532nm) TCS (840nm)	For use in initial alignment For use in Hartmann camera	Specified mirror reflectivity at specific wavelengths
Substrate and coating bulk mechanical & chemical quality	SYS	IFO thermal noise from substrate fluctuation-dissipation	Minimize substrate and coating loss angles.
Substrate dimensions			Choose high internal mode resonant frequencies
Secondary surface AR reflectivity & wedge angle	SYS	Stray light beam control and scattered light noise	Generate ghost beams from secondary surfaces
		Wedge astigmatism	Signal loss due to astigmatism
AR reflectivity & wedge angles	ISC	Signals for length and orientation control servos	Select ghost beams of desired properties
ETM residual transmission			
Mean surface reflectivity	SYS	Optimum IFO operation parameters	Specific mirror reflectivity values
Surface reflectivity tolerances		Contrast defect	Coating uniformity
Element surface contamination control (cleaning, handling)	SYS	IFO sensitivity degradation	Lowering of Qs Increased light scatter
		Advanced LIGO down time	Damage of optical surfaces
RC beam expansion and matching	IOO	Optimum IFO operation parameters	Efficiently match arm cavity mode to PRM and SRM

## 4.2 Characteristics

### 4.2.1 Performance Characteristics

The discussion of the COC requirements will be broken down into the following characteristic areas:

- Physical Size and Shape.
- Mechanical loss.
- Matching to Interferometer parameters.
- Distortion of the wave front: light scattering (including birefringence)

- ⇒ Matching losses
- ⇒ Prompt loss.
- ⇒ Diffraction due to finite TM size
- Absorption (losses): thermal effects.

## 4.2.2 Physical Characteristics

Requirements on the COC follow a nominal physical prescription as summarized in table 2.

### 4.2.2.1 Size and Shape (LIGO-M050397)

The exact right circular cylindrical geometry is required to be slightly altered as follows:

- Edges are to be 45° chamfered (face width = 2.0±0.3mm) in accordance with standard optical fabrication safety practice (reducing the face diameters from the cylindrical diameters).
- Each surface will have a wedge angle with respect to the cylindrical axis for ghost beam aiming, to suppress stray light, to facilitate pick-off of signals for servo control and to sufficiently separate surface reflections for high quality metrology.
- The BS wedge angles are small (in proportion to this element's necessary thinness).
- The ITM, ETM, PR3, and SR3 primary, HR, surfaces will be spherical concave. All secondary (AR and BS) surfaces are taken to be nominally flat. Current design calls for a convex SRM and PRM.
- Flat areas are required on the cylindrical sides of all Test Masses, all other optics are cylinders.

#### 4.2.2.1.1 Diameter and Thickness

The Test Masses are required to weigh 40 kg in order to meet the Advanced LIGO detection sensitivity goals. The diameter and mirror radii of curvature are selected to minimize TEM<sub>00</sub> mode diffraction loss and thermal noise. We assume a clear optical aperture 0.6 cm in diameter less than the physical substrate diameter to allow for suspension settling beam centering tolerance, and mirror face safety margin chamfer plus coating edge tolerance. The aspect ratio is chosen to ensure sufficiently high internal mode frequencies.

##### 4.2.2.1.1.1 Beam Splitter (LIGO-M070120)

In LIGO I the single pass geometrical (clipping) loss for the beam splitter was required to not exceed 20 ppm, so that it does not significantly scatter the PRC cavity mode. This criterion nearly be met for the Advanced LIGO choice of 370 mm diameter BS substrate (364 mm clear aperture) and ITM beam radius = 5.55cm (RC total loss dominated by AR coating reflectivity and internal telescope diffractive loss). However the SRC involves different somewhat higher loss [ray] paths (see T1000226-v2, T0900326-v2, P080004, but note sensitivity to associated baffling in T1000090-v3) Because of its use as a diagonal optical element the BS can induce astigmatism in two ways: first, in transmission if it is wedged, even if it is otherwise a perfect prism. Second, any spherical

non-flatness will induce reflected [primarily] wave-front astigmatism (T0900384-v1). The mean lensing effect can be CP compensated, however the induced astigmatism cannot and is therefore discussed separately in 4.2.2.6.

#### 4.2.2.1.1.2 Test Masses

The test mass diameter is chosen to be as large as technically feasible and consistent with having no internal normal modes below 5 kHz. The radii of the beams at the test masses will be chosen so that the 1 ppm (exact Gaussian) energy contour lies within the diameter of the optic.

#### 4.2.2.1.1.3 Recycling Mirrors (LIGO-M070055)

The RM diameter is chosen to accommodate a small optics (e.g. input mode cleaner) suspension design. This requirement follows from the assumption of stable RC design, with their concomitant small ( $< 2\text{mm } w_{\text{RM}}$ ) input beam spots.

#### 4.2.2.1.1.4 Telescope Mirrors

The requirement that the RC cavities both be of a stable design necessitates additional intra-cavity optics (“focusing telescope”). The candidate design (LIGO-T080075-01) stipulates a two HR mirror configuration for this telescope. Exact parameters for these may still change in inessential ways. IFO control and alignment signals are required via PR2 (for input MMT alignment, PSL intensity stabilization) and SR2 (for output MMT alignment and an entry port for the ITMy Hartmann sensor beam) residual transmission. This requires sufficient OPD and surface 2 polish and coating quality for these optics.

#### 4.2.2.1.1.5 Compensation Plates (CP) (LIGO-T1000175 Thinner Compensation Plates...)

The CP plates are both surface AR coated FS plates. The CP principle role is to compensate for the beam absorption (mostly HR) induced lens in the ITM. To best accomplish this it must have minimal beam absorption itself. Therefore it is required to be fabricated from ultra low 1064 nm absorbing FS. We specify  $< 0.2$  ppm/cm absorption for the CP in the understanding that such material is possible to produce.

**Table 2 Physical Parameters of Interferometer COC**

Physical Quantity	Test Mass		Splitter	PRM SRM	CP Plates	PR/SR	
	ETM	(ITM)				2	3
Diameter of substrate $\phi_s$ (mm)	340		370	150	340	<265	<265
Optic Thickness $h_s$ (mm) at wedge Max	200		60	75	100	101.4	101.4
1 ppm beam power contour diameter (mm)	326	292	410 major	10.5 min	292	292 max	292 max
Lowest internal mode frequency (kHz)	5.97		6.3	>100	6.1	NA	NA
Weight of Suspended Component (kg)	40		13	~3 max	20	~3	12

Wedge angle	<0.1°	0.08°	0.04°	< 2.0°	0.08°	2.0°	0.6°
Surface 1 [concave] radius of curvature (km) and g+ factor	2.245 g <sub>2</sub> =-.8233	1.934 g <sub>1</sub> =-1.0268	Flat, >200	See table 3	Flat	See table 3	See table 3

#### 4.2.2.2 Internal resonances, Qs, thermal noise and quantum limit.

##### 4.2.2.2.1 Quantum limit.

What is termed the standard quantum limit for IFO sensitivity depends on the mass of the test masses. Test Masses are required to be 40 kg for optimum sensitivity given the maximum design 0.85 M Watt interferometer circulating arm cavity power.

##### 4.2.2.2.2 Thermal noise

Only the thermal noise of the TM substrates will be considered here since the contribution of the other COC is much less important. The TM's thermal motion can be modeled using Levin's theorem, and will depend on the mechanical loss of the substrate material, the coating, and any attachments to the optic. Internal normal modes of the optics will be designed to be out of the gravitational wave band.

###### 4.2.2.2.2.1 Substrate mechanical and thermal properties

The mechanical loss angle relevant to thermal noise calculations for fused silica, which will depend on the choice of axis, the intrinsic loss of the substrate, and any surface loss will be less than  $10^{-7}$  in the frequency band where mirror thermal noise is a major contributor to Advanced LIGO noise (below 300 Hz).

The specification is stated in terms of loss angle rather than Q. This is because the thermal noise will be determined by the loss from a specific distribution of energy, namely that of the static Gaussian pressure specified in Levin's theorem. While measuring a modal Q is a rough guide to the expected thermal noise, the parameter of interest is the effective loss angle to be used in Levin's theorem. Mechanical loss has also been found to be a function of frequency in fused silica, and modal Q's are measured at frequencies well above 300 Hz.

###### 4.2.2.2.2.2 Coating mechanical, optical and thermal properties

The optical coating will be chosen so that the combined Brownian thermal noise, calculated with the Nakagawa/Gretarsson formula, and the thermo-optic (combined thermoelastic and thermorefractive) noise, calculated from the Evans formula, will be no more than  $5.7 \times 10^{-21}$  m/Hz<sup>1/2</sup> per optic at 100 Hz. This will be affected by the coating mechanical loss, its Young's modulus, thermal conductivity, and other mechanical and thermal properties. The coating must also satisfy an optical loss and scatter requirements specified in Section 4.2.2.5

The coatings will have their layer thicknesses optimized to give minimum thermal noise but still meet the reflectivity requirements. This will be done using an algorithm developed at the

University of Sannio and depends on having good input parameters for the coating mechanical loss, Young's modulus, and  $dn/dT$ . A prototype optimized coating made from tantalum and silica has been measured in the Thermal Noise Interferometer. The exact choice of coating layer thicknesses will be made by the vendor, but will be done to meet the reflectivity requirements at 1064nm and 532nm as well as minimizing thermal noise. This choice will be made in close consultation with LIGO and LSC scientists.

#### 4.2.2.2.3 Substrate diameter and thickness

These dimensions determine the mode resonance frequency spectrum and also influence the thermal noise. The choices of shape and aspect ratio determine an initial mode sequence. These Test Mass resonances should occur at the same frequency and be above 5 KHz. Shape perturbations (face wedges, bevels, substrate imperfections) are assumed to not significantly modify the spectrum. The dimensions that satisfy the mode frequency requirement are in an acceptable range for thermal noise.

#### 4.2.2.2.4 Attachments and contamination

Any contacting material (coatings, contamination, etc) or coupling to external systems (SUS) can cause increased thermal noise. The contribution to thermal noise, due to the loss angle and Young's modulus of any contacting material, must not exceed 1/10th of the thermal noise of a pristine optic.

### 4.2.2.3 Matching to SYS IFO parameters

The overall optical design of the IFO depends on the average effective optical characteristics of each optical surface on which the circulating nominal  $TEM_{00}$  beam impinges. A key SYS requirement is for low [as possible] arm cavity round trip  $TEM_{00}$  mode loss ( $\mathcal{L}_A$ ). Key design emphasis will be on achieving mean  $\mathcal{L}_A \sim 75$  ppm, with a worst case limit being twice this ( $\sim 150$  ppm/arm). Characteristic *matching*, for instance of  $TEM_{00}$  mode shape parameters, cavity finesse and  $\mathcal{L}_A$  between the two IFO arms then follows as a strong secondary requirement (LIGO-T070247-01 (2.2.5)).

#### 4.2.2.3.1 HR-ITM reflectivity

The SYS requirement is that mean arm cavity finesse should be 450 (low finesse option), corresponding to ITM  $R \sim 1 - (.014)$ . The differential  $1 - R_{ITM}$  match must be such that it is possible to fabricate at least five pairs of mirrors, such that for each pair  $2(T_1 - T_2)/(T_1 + T_2) < 0.01$ , where  $T_1$  is the maximum and  $T_2$  is the minimum mirror transmission. Such matching assures that the net differential arm loss would be dominated by HR surface scatter [loss] when the arm to arm scatter loss attains the requirement limit of  $\Delta\mathcal{L} < 35$  ppm.

#### 4.2.2.3.2 HR-PRM transmission

The current best informed 1064 nm Bench and FFT model runs yield an optimized transmission for the HR-PRM coating near 0.03. A tolerance of at least  $\pm 0.003$  will be required for any ultimately selected transmission value. For example figure 3 of LIGO-T070247-01 show that lost coupling due to this tolerance becomes  $<$  the uncertainty in likely arm cavity loss. It is anticipated that PRM HR reflectivity will remain an open parameter to be selected and ultimately matched to accommodate actual installed arm cavity loss and selected finesse. The COC required [for this design document] call for physically small ( $\sim$ input MC) RM and concomitant suspension. This will

allow multiple PRMs (with tailored reflectivities) to be fabricated, and easily changed out to optimize IFO performance.

#### 4.2.2.3.3 HR-SRM transmission

An optimized transmission for the HR-SRM coating is 0.2 (consistent with science modes 1-4 of LIGO-T070247-01-I). A tolerance of at least  $\pm 0.01^{\text{TBD}}$  should be required. Advanced LIGO anticipates using various SR strategies with widely varying specifications. These remain under study, however the present SRC design calls for physically small ( $\sim$ MC scale) SRM and concomitant suspension. This will facilitate various SRMs to be subsequently fabricated to match IFO optical performance and GW search sensitivities.

#### 4.2.2.3.4 HR-ETM transmission

The HR-ETM would nominally have unit reflectivity. However a small leakage transmission is desired in order to aid in locking and IFO monitoring. The transmission should also be small compared to the dominant cavity loss mechanism, which is scattering loss due to the cavity mirror surface quality, of order  $> 25$  ppm per surface. The requirement is  $5 \pm 1$  ppm, which satisfies the requirement compared to scattering loss, and allows enough light to transmit through for diagnostics, and is compatible with coating technology. For details see T010075-v3.

#### 4.2.2.3.5 AR coating reflectivity

In order that the ghost beam loss from the recycling cavity AR coated faces (surface 2) be small compared to the arm cavity (visibility) loss their reflectivity should be  $\leq 50$  ppm with a best effort to achieve  $< 20$  ppm. Allowing a large margin, this AR loss limit is consistent with required RC total loss budget (section 4.2.2.6). This bound can still provide for reasonable diagnostic (assuming the low power modes described in 1.3 of LIGO-T070247-01) signal level (see 4.2.2.7.4), and allow a coating design whose reflectivity is inherently insensitive to surface position variations of coating layer thickness. The ETM AR coating is required to be  $< 500$  ppm at 1064 nm, which allows for light to transmit through for diagnostics, and between 0.1% and 2% at 532 nm, which allows for the lock and alignment interferometer.

#### 4.2.2.3.6 HR-BS coating

The HR-BS coating must perform a beam splitting of  $45^\circ$  incident light (P polarized) such that the exit beams are equal in power within 1% (including the effects of absorption and the AR-BS coating). See appendix D.3 of E950099-04-D. The obverse BS side coating must also be at AR minimum with respect to P polarization.

#### 4.2.2.3.7 Effective TM curvature radii

The TM radii of curvature are determined by the desired Gaussian  $\text{TEM}_{00}$  beam mode size (at TMs) prescribed by SYS. Radii of curvature with negative  $g (= 1 - L_{\text{ARM}}/R_{\text{eff}})$  values near the cavity mode stability threshold ( $\sim 2000m$  for LIGO 4000m cavity length) are required for TM mechanical angular stability with respect to radiation pressure. Large transverse mode size (as  $R_{\text{eff}} \rightarrow 2000m$ ) is desired to mitigate mirror thermoelastic noise, but cannot be so large that finite  $\phi_{\text{mirr}}$  edge diffraction loss limits the IFO signal extraction efficiency. In practice a requirement on TM  $\phi_{\text{mirr}} < 34$  cm is placed by LIGO-T040199-00. Given this reasonable constraint, optimum mode sizes can be determined by IFO optical field simulation (summarized in Figure 1). For the arm cavities alone a symmetric ( $w_{\text{ETM}} = w_{\text{ITM}} \sim 6.0\text{cm}$  point in figure 1) mode would be optimal. Detailed simulations

of losses within the stable RC of table 3 matched to the arm cavity show substantial additional loss. This is ameliorated by choosing a slightly asymmetric arm mode design ( $w_{\text{ETM}} = 6.2$  cm;  $w_{\text{ITM}} = 5.3$  cm point corresponding to  $R_{\text{eff}} = 2245$ m and 1943m for ETM and ITM) at the cost of slightly increased mirror thermal noise. The gradient in thermal noise (higher in the direction of smaller beam spots) is clearly balanced by an opposite trending gradient in diffractive signal loss (higher for larger beam spots).

Requiring, then, an IFO arm cavity operating point of  $R_{\text{eff}} = 2245$ m and 1943m for ETM and ITM, we can specify the cold polished surface 1 fabrication ROC. A tight but reasonable fabrication tolerance on  $R_{\text{eff}}$  would be  $\pm[\Delta R_{\text{tol}}] = \pm 10$ m (out of  $\sim 2000$ m). A box representing such variation is illustrated in fig. 1. Note that the TCS ring heaters (for each TM) have sufficient authority to compensate for such a tolerance range. However here we adopt the constraint that the interferometer be operated at optimum sensitivity at low power with no initial TCS compensation. In this case being at low  $w_{\text{TM}}$  corner of the tolerance box could degrade performance. To avoid this, a bias for specified  $R_{\text{eff}}$  such that  $R_{\text{spec}} = R_{\text{eff}} - [\Delta R_{\text{tol}}]$ , will always allow for consistently (marginally !) higher initial sensitivity. Low power operation favors this direction of bias (e.g. BBH range increases fractionally  $\sim$ twice as much at 20W, wrt 125W, with  $R_{\text{eff}}$  reduced by 10m). The magnitude of bias (no more than 10m) is still well within a incrementally linear regime of extrapolation (e.g.  $\sim$ within Fig. 1) and far from cavity instability ( $R_{\text{eff}} - 90$ m). Note also that the sign of this bias is such as not to diminish the effective range of the TCS ring heaters, and yet its magnitude is small compared to the anticipated full power beam heating effect.

Since TCS ring heaters are implemented on all four TMs it is assumed that any  $R_{\text{eff}}$  variations due to fabrication *reproducibility* can be adequately compensated by these heaters (see section 4.2.2.7). This compensation should work well at high power where a certain degree of TCS correction will always be required. Again, this will not necessarily hold at low power/no TCS, where reproducibility tolerance,  $\Delta R_{\text{rep}}$ , would have to be tighter.

We estimate that  $\Delta R_{\text{rep}} < \pm 3$ m must attain to keep differential arm mode CD to less than  $10^{-4}$ . We note here that SIS studies have indicated a high sensitivity of online/offline cavity beam throughput to associated COC optic baffle clipping losses. It is therefore incumbent on the AOS design of these baffles to not significantly impact the “bare” COC performance (e.g. CD, see T1000090-v3).

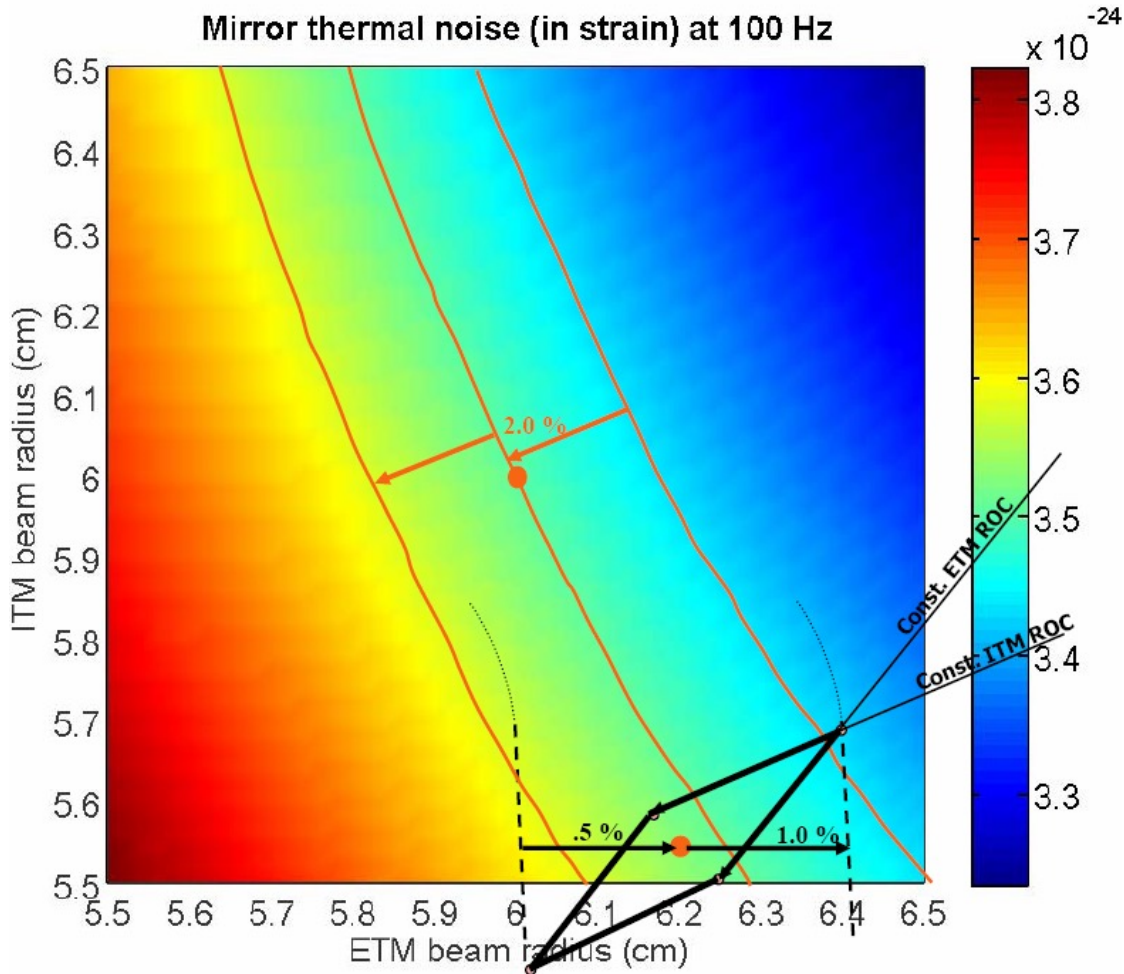


Fig. 1 Principle IFO S/N dependencies as a function of TM  $R_{\text{eff}}$  (in terms of  $w_{\text{TM}}$ ). In color relief is the dependence of thermo-elastic noise (@ 100Hz), with gradient steps of 2% in IFO S/N at full power. A similar gradient of relative  $\text{TEM}_{00}$  field signal diminution dominated by arm cavity diffractive loss is indicated (fractional wrt 75ppm net arm RT loss) by the dashed black lines. Note that near the chosen asymmetric operating point diffractive loss is significantly dependent only on  $w_{\text{ETM}}$ . The trapezoid about this operating point is the +/-10m error box in ETM and ITM  $R_{\text{eff}}$ .

#### 4.2.2.3.8 PRM and SRM effective curvature matching.

The telescopic PRC and SRC put moderate requirements on the absolute  $R_{\text{eff}}$  for the PRM and SRM. The candidate RC telescope design (LIGO-T080075-01, table 3 and most recent T0900043-v11) transforms a required ITM beam wave front curvature matching tolerance of <1% to a mean RM surface 1  $R_{\text{eff}}$  tolerance of 2.5% (essentially *absolute* since the ITM  $R_{\text{eff}}$  is absolutely constrained per section 4.2.2.3.7). However, since practical RC telescopes will not be *constructed* (let alone *known*) to absolute specification, this problem will necessarily be relieved by having an appropriate length [matching] adjustment within the telescope (+/- 10cm adjustment in P/SR2 with concomitant +/- 20cm change in P/SRM position, T080198, T0900043-v10, P080004-P). Since anticipated adjustments will be to small optics (with wire pendula), this is planned (in concert with SUS) to be accomplished by translation of their entire SUS towers. The final design of these elements, in concert, can be chosen to allow this flexibility. Since this absolute *mean* adjustment is

likely to be taken in preliminary setup, changes of matching during operation must be separately considered. These can occur either due to beam heating (for FS the PRM *local*  $R_{\text{eff}}$  will change  $\sim 0.6\%$  from cold to full power (10ppm HR absorption) for the “low finesse” arm cavity choice), or due to surface finish irregularities (making the RM have different  $R_{\text{eff}}$  for shifted beam spot positions). In any case this specification and the  $R_{\text{eff}}$  variation with beam power are well within the compensation range of the TCS CPs ( $>25$  larger, but in one direction of matching only). The ITM thermal lensing and RM HR thermal change are not compensating effects. Other options include fabricating the RMs of ULE glass, and furnishing some [common] RC element with a ring heater.

From T0900043-v11 See design and rationale therein

Optics	ROC (m)		Beam Size (mm)		Sag ( $\mu\text{m}$ )		ROC Tolerance in % and mm			Tol. Sag (nm)	
	Straight	Folded	Straight	Folded	Straight	Folded	Both (%)	Straight (mm)	Folded (mm)	Straight	Folded
PRM	-11.00	-8.87	2.2	2.1	-0.23	-0.24	1	-110.0	-88.7	-2.3	-2.4
PR2	-4.56	-4.41	6.2	6.3	-4.18	-4.54	0.5	-22.8	-22.1	-20.8	-22.6
PR3	36.00	34.00	54.0	54.5	40.46	43.62	0.5	180.0	170.0	201.3	217.0
SRM	-5.69	-11.40	2.1	2.6	-0.38	-0.31	1	-56.9	-114.0	-3.8	-3.0
SR2	-6.43	-4.89	8.2	6.6	-5.27	-4.47	0.5	-32.1	-24.5	-26.2	-22.3
SR3	36.00	36.00	54.0	54.2	40.50	40.80	0.5	180.0	180.0	201.5	203.0

#### 4.2.2.3.9 Coating performance for ancillary wavelengths

The system design of advanced LIGO incorporates light beams at other wavelengths than the principle interferometer carrier of 1064nm (and its RF sidebands) which share significant portions of the interferometer optical path. One, at 532nm, is designated for the ISC lock acquisition. The TCS Hartmann wavefront sensing system is the other, operating at  $\sim 840\text{nm}$ . This requires (see table 1) various COC coatings to be operationally compatible at these ancillary wavelengths with the design of their associated systems. Exact optimization of coatings in all cases is still under analysis and refinement (see C1000029, C1000140, C1000417, and C1000251).

#### 4.2.2.4 Distortion of the wave front: Modal Distortion

Imperfections of the COC surface profiles, their finite diameter, as well as the combined influences of the substrate, coating and bulk index and birefringence inhomogeneities, as well as localized material structural or contamination “point” defects contribute to distortion of an ideal  $\text{TEM}_{00}$  mode wave front propagating in the IFO. All such distortions may be regarded as scattering losses (to HTMs). In this section only the influence of scatter on sensible distortion of the arm cavity mode field is considered. For example distortions (discussed in the previous sections) which alter  $R_{\text{eff}}$  of the TM surface 1 change the mode mean  $w_i$  predictably. For this particular example it is assumed that  $R_{\text{eff}}$  can be suitably TCS controlled such that this modal distortion is compensated. Light lost from the cavity mode via scatter is considered in 4.2.2.5. Table 4 summarizes required limits to these distortions.

It has been proposed that metrology data on and requirements for mirror surface quality be unified solely in the form of PSDs. This approach has great appeal in that reflected wavefront distortions are represented in single curves which can conveniently be compared to others. There is simply more information contained in the PSD curve than any set of partial rms values. This issue has been grappled with since the LIGO I pathfinder era. Indeed as an invaluable aid we now routinely use as much data as possible in the form of PSDs. On the other hand it has major technical and interpretational limitations allowing risk in its unified use for setting requirements.

It is important to categorically distinguish COC [surface, in particular] distortions to accurately quantify, most importantly, cavity loss, then also cavity modal distortion leading to coupling inefficiencies (“mismatch”). PSDs do not distinguish these effects. Further, the PSD, being a Fourier decomposition, very poorly represents the very lowest order “matching” distortions. This is why, from the outset, data usually has such low order distortion terms subtracted out before even being represented in PSD form. But which terms ought to be separated out [subtracted]? Or, equivalently, down to what frequency should the PSD be used? In principle there is no resolution to this, essentially the reason FFT simulation of the full spatial data has come to be relied on.

Still it might be argued that the PSD could be used to best describe [cavity] loss. Certainly this holds well within the regime of micro-roughness ( $\lambda_s \ll w_{TM}$ ) where features are of random orientation and the loss is accurately proportional to the area under the PSD. In our regime of surface quality the PSD is steeply rising with  $\lambda_s$ . Therefore total loss becomes ambiguous to extract from integrated PSD as the integration limit  $\lambda_s \rightarrow w_{TM}$  is approached. Recently FFT studies have shown a deeper ambiguity. Randomly generated mirror distortion maps constrained to the same PSD (therefore same surface rms) are found to cause net cavity losses differing by large factors (see LIGO-G080084-00, slide 10). Further study of this effect has shown that it is mid scale,  $\lambda_s < w_{TM}$ , surface aberrations which are individually responsible. One particular “real” mirror map (an Advanced LIGO pathfinder) has been used in simulation which clearly shows anomalous loss (loss strongly dependent on subtraction of one aberration term far out of proportion to its rms<sup>2</sup>). Further simulation and analysis in this regard is contained in T0900306-v6 and T080392-v1.

#### 4.2.2.4.1 Large $\lambda_s$ errors.

Sufficiently large  $\lambda_s$  mirror figure deviations will perturb the arm mode from the nominal TEM<sub>00</sub> Gaussian/spherical profile. For  $\lambda_s < \text{few cm}$ , scatter of the TEM<sub>00</sub> field is substantially lost from the arm and will not cause sensible cavity mode distortion in our high finesse regime. Distortion  $\lambda_s > 2 w_{TM}$  (~12 cm) are unimportant since beam scatter does not occur beyond this scale (affects R<sub>eff</sub> perhaps astigmatically). Distortions within this limited  $\lambda_s$  band can only excite some few lowest cavity HTM orders ( $n < 10$ , where n counts the HTM Guoy phase multiple). For a given specification of surface “figure” deviation (taken here to be rms,  $\sigma_F$ , deviation from R<sub>eff</sub> sphere over the mirror central  $3w_{TM}$  diameter,  $\phi_F$ ) the limit for any one HTM distortion saturating this specification may be calculated. The largest case distortions then estimate possible degradation to IFO performance. As a working example we use the stringent but achievable specification  $\sigma_F < 0.7\text{nm}$ . The most critical implications of this specification occur in its application to the arm cavity HR surfaces. For all other COC optical surfaces no tighter a specification is anticipated, with individual design cases still under refinement (see Opt. Exp. **16**, 10018).

One consequence of this perturbative mode distortion not yet fully analyzed is increased arm cavity mode diffractive loss. It is anticipated that any contamination of the  $TEM_{00}$  mode by HTM components will generally increase the effective beam transverse size, and hence its diffractive loss due to the finite mirror diameter. The very small HTM contaminations concomitant on  $\sigma_F < 0.7\text{nm}$  cause only second order diffractive loss changes, so are neglected. Likely,  $n < 8$ , HTM contaminations have been calculated, in clipping loss approximation, and found to increase cavity loss by  $< 10$  ppm (extreme worst case). A true quantitative estimation of loss in this diffractive regime (including also well into the prompt regime 4.2.2.5.1)) comes from FFT arm cavity simulations (up to date summaries in T080392-v1, T0900306-v6, T0900159). Mirror distortion maps of constant residual  $\sigma_F$  (e.g. 0.7 nm) randomly generated within an estimated super-polish PSD form (see LIGO-G080084) show typical cavity loss somewhat higher than allowed by the section 4.2.2.5.3 entry in the budget table 5 (however well below saturating the prompt loss bound, 4.2.2.5.1, for  $\sigma < 0.7\text{nm}$ ). Then also, one Advanced LIGO PF optic's metrology map has been the basis for arm cavity FFT study. If its lowest order aberrations are subtracted (known not to appreciably affect  $\mathcal{L}_A$ ) and its map is scaled down to 0.7nm rms the FFT loss incurred is  $\sim 5\text{ppm}$  (then reasonably allowing 2x this for a cavity of two similar mirrors).

The remaining consequence is mismatch of the distorted arm mode(s) to the mean "carrier"  $TEM_{00}$ . This has two effects. The first is HTM  $CD_{HTM}$  due to the generally different modal distortion content between the two arms. This is discussed in 4.2.2.4.4. The second is the direct diminution of GW SB signal due to  $TEM_{00}$  dilution.

Each arm will develop a perturbatively different resonant carrier mode. The contaminating HTM modal field content will be at most  $\sim \text{order}[2\pi\sigma_F/\lambda] \ll 1$  where the exact coefficient depends in some detail on the individual HTM saturating the surface distortion  $\sigma_F$ . In this perturbative distortion regime, then, the diminution to the  $TEM_{00}$  field will be only  $\sim \text{order}[2\pi\sigma_F/\lambda]^2$ . It is assumed that this small mismatch diminution of the carrier is always practically compensated with IFO input power. However any GW SB field generated in this cavity will be in this same distorted mode and suffer the same dilution. This second order diminution has been calculated exactly for Gaussian HTM modes of order  $n < 8$  for the nominal arm cavity parameters. The largest fractional [field strength] diminution found for any one HTM saturating the  $\sigma_F = 0.7\text{nm}$  specification was  $< 200$  ppm. This is entirely negligible with respect to the diminution of GW SB field due to scatter loss in the arms  $\sim \mathcal{L}_A G_{Arm}/4$  as high as  $\sim 7500$  ppm (see section 4.2.2.5).

#### 4.2.2.4.2 Transmission OPD errors

Transmission OPD errors, either from bulk or thickness distortions can similarly perturb the  $TEM_{00}$  mode in the RCs. It might be imagined that the CP correction could restore mode purity (say undistort the arm cavity mode GW SBs on their way to the AS port) simultaneously with its primary role of correcting for the ITM and BS bulk thermal lensing. This can be achieved but only in the phase front quadrature. General arm cavity mode distortions will be both in phase and amplitude quadratures, the later being uncorrectable by the CP.

FS blanks suitable (in size and bulk 1064nm absorption) for advanced LIGO ITM BS and CP are understood to be available with [cold] refractive index inhomogeneity  $\delta n/n < 0.5$  ppm (P-V). If longitudinally coherent through an ITM this would result in a worst case wave front distortion  $0.1\lambda$  or about 100 times found acceptable for the arm mode distortion in the previous section. Very closely the typical inhomogeneity is distributed as an optical power (or at least varies as very large

$\lambda_s$ ) phase distortion of magnitude much smaller than the CP is designed to be capable of removing. However during material acceptance and subsequent optic fabrication such power distortions will be monitored (by measurement of the central  $\sim 1.5 w_{\text{ITM}}$  radius phase front as it is reflected from surface 1 through surface 2) and surface 2 polish compensated during the ITM, BS and CP polishing. It is this final fabrication compensated OPD specification that appears in table 4. The deviation in OPD power is comparable to the allowable change in radius of curvature of the Test Masses (+/- 10 meters).

Present design calls for neither this power compensation polish nor thermal lensing compensation for the ETM. This will leave a possible large, predominantly spherical, uncorrected distortion in the ETM transmitted monitor beam. An appropriate grade of FS has been chosen to minimize higher order OPD distortions. ETM/reaction mass OPD distortion is analyzed in LIGO-T080073-01 and M080042-00.

#### 4.2.2.4.3 Birefringence Effects

Birefringence effects have been considered by Winkler, et al (2.3.2) These may be: intrinsic, heating strain induced, or mechanical stress induced. We place a nominal requirement on intrinsic material birefringence, however the thermally induced effects are expected to dominate by a large margin. These effects have been studied and found small compared to dominant beam heating OPD phase distortions, correctable by the TCS CPs. To the extent that residual FS birefringence is small, any spatially non-uniform attenuation will be at negligible second order.

The native (cold, unsuspended) FS considered for use in the critical transmissive optics (BS, ITM) has typical residual birefringence which would at most rotate polarization along the beam propagation direction by  $<.04$  rad (P-V) through an ITM. Distortion to the TEM00 mode would only be second order in this rotation angle, so is an acceptable requirement.

#### 4.2.2.4.4 Contrast Defect loss.

The minimum intrinsic  $CD_c$  for the signal mode will result predominantly from imbalance in the TEM<sub>00</sub> mode arm to arm cavity loss. The SYS requirement on the differential arm internal RT loss is  $\Delta\mathcal{L}_A < 35\text{ppm}$ . This will result in  $CD_c < 10^{-5}$  for a low finesse arm cavity choice. This requirement may be regarded as stringent depending on the overall achievable  $\mathcal{L}_A$  budget, as discussed in section 4.2.2.5.3. Here we discuss (see also 4.2.2.1.1.1) only COC contributions to CD, and not any SUS or AOS (baffle clipping or alignment tolerancing) contributions. The inherent asymmetry of the BS within the P/SRC may contribute significant CD (extensively analyzed and shown manageable in T1000090-v3).

Here we estimate  $CD_{\text{HTM}}$ , the contrast due to all other HTM distortions imbalanced arm to arm, which substantially remain within the COC aperture. Expecting these to be the same set of low order HTMs considered in 4.2.2.4.1 we estimate the  $CD_{\text{HTM}}$  expected from individual HTM saturation of the  $\sigma_F$  bound. This is entirely taken as the real quadrature (amplitude) distortion contamination. All imaginary (phase) quadrature distortions reflecting from the arm cavities are assumed to be suppressed by CP correction. In this situation the same modal amplitudes contribute to  $CD_{\text{HTM}}$  as contributed to the cavity mode distortion of 4.2.2.4.1. With the additional conservative assumption that there is no anti-correlation between arm distortions, the bound from single HTMs saturating the  $\sigma_F$  requirement in each arm is  $CD_{\text{HTM}} < 5 \cdot 10^{-4}$ . Experience with LIGO I indicates that CD is a small fraction (few  $\times 10^{-4}$ ) of the total carrier IFO loss. This is of the same order loss ( $\sim$ several 100s ppm) as that allocated for RC AR coating/pick-off losses: entirely negligible.

**Table 4 Required limits on sources of wave front distortion (surface 1)**

Document section	Requirement	Test masses		Beam splitter, Fold mirrors	Correct Plates	S/PR telescope mirrors	S/PR mirrors
4.2.2.3.7	Cold arm-arm match (fractional wrt $R_{\text{eff}}$ at mirror)	0.0015	0.0015	0.001 wrt flat	.002 (flat)	TBD*	N/A
4.2.2.3.8	RC to arm match $R_{\text{eff}}$ (fractional)	N/A	N/A	N/A	.002	TBD*	.001
4.2.2.4.1	Rms surface errors for $w > \lambda_s > 2$ mm out to $\sim 3w$ diameter	<0.7 nm	<0.7 nm	< 2 nm	< 3 nm	TBD*	< 2 nm
4.2.2.4.6	Rms surface errors for $\lambda_s > 2$ mm past $\sim 3w$ diameter	2.5 nm	2.5 nm	3 nm	< 4 nm	TBD*	> 3 nm
4.2.2.5.1	Rms surface micro-roughness (see section text) out to $\sim 3w$ diameter	<0.2 nm	<0.2 nm	<0.5 nm	< 2 nm	TBD*	< 0.5 nm
4.2.2.4.6	Rms surface micro-roughness (section 4.2.2.5.1 text) past $\sim 3w$	1 nm	1 nm	1 nm	< 4 nm	TBD*	1 nm
4.2.2.4.2	Rms transmission OPD for $\lambda_s > 1$ cm out to $\sim 3w$ diameter	< 8 nm	< 400 nm	< 8 nm	< 8 nm	TBD*	< 50 nm
4.2.2.4.3	Birefringence (transmission) Rad.	0.04	N/A	< 0.02	< 0.03	NA	< 0.04

\*Note: design of the S/PR telescope configuration has significantly evolved. For up to date details see current documentation in LIGO-T0900043-v11.

#### 4.2.2.4.5 Central errors

With the high optical quality TMs we anticipate the cavity mode intensity profile will be closely Gaussian out to the edge for an accurately aligned (beam centered) IFO. Then only the central portion of the HR surface will substantially determine the cavity performance. A distinct specification for a central portion with respect to the remaining, peripheral, portion is important for fabrication practicality. FFT simulations of the effect of mid to large  $\lambda_s$  distortions indicates that “central” may conservatively be taken to be within a radius  $< 1.5 w_{\text{TM}}$  (encircling 99% of the aligned mode power). It is clear that scattering prompt loss (see below) from distortions  $\lambda_s \ll w_{\text{TM}}$  will proportionally be taken into account over this central region, and therefore need only be critically specified there. It is further assumed that this power weighted proportionality will also approximately apply on all other  $\lambda_s$  distortion scales (excepting  $R_{\text{eff}}$ ).

#### 4.2.2.4.6 Peripheral errors

Only 1% of the beam energy lies outside of  $\phi = 3w$ . It is therefore expected that surface imperfections in this periphery will contribute much less to loss from the effective cavity mode power. This is borne out by FFT modeling which is the basis for the requirement values. Therefore we may anticipate relaxing specification of optical surface errors by a large factor in this peripheral zone. Since this zone comprises  $\sim 75\%$  of the TM optically finished face, this relaxation can

substantially reduce the fabrication cost and difficulty. Critical relief in optical fabrication is had in relaxing the mid to large  $\lambda_s$  distortion rms specification by a modest factor (<2.5 nm rms requirement, Table 4).

### 4.2.2.5 Distortion of the wave front: scattering losses

The arm cavity mode defined in the previous section will suffer effective loss as it circulates, most critically in the arm cavities where  $\mathcal{L}_A$  directly limits the potential IFO optical gains and efficiency. The entire budget of these losses is set out here (green highlight in table 5) along with required limits. Loss to the arm cavity mode due to prompt (meaning that it does not sensibly further distort the mode as discussed in 4.2.2.4.4) imperfection scatter dominates the budget. Lesser sources due to residual  $T_{\text{ETM}}$  transmission and coating absorption are included to complete the budget. Since both the fabrication investment and difficulty are highest for the TM optics only the specific requirements for these are examined (unless specifically stipulated otherwise). It is assumed that other optics can at least as easily/cheaply be produced to these same requirements, or individual specifications relaxed in obvious ways on a case by case basis.

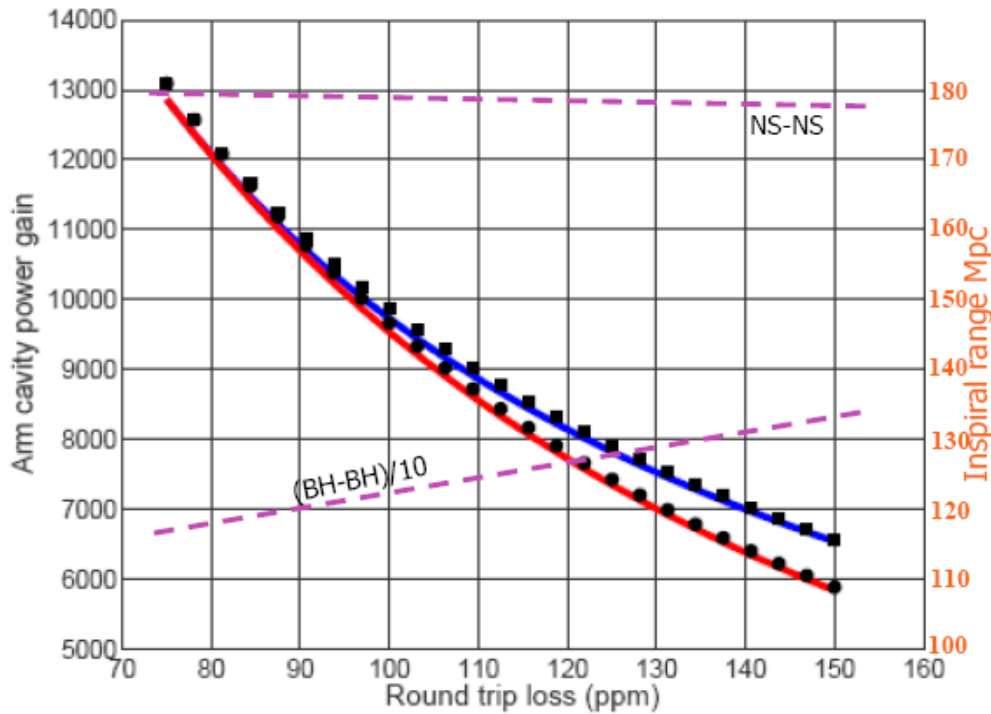


Figure 2 Influence of round trip arm cavity fundamental mode loss on the interferometer performance. Dashed curves show the dependence of net (integrated) inspiral range. Note that BH-BH range improves with loss since the cavity power and thus radiation pressure noise decreases improving low frequency SN. The blue curve is maximum arm power for fixed ITM transmission (0.014) while the red is for optimized (at each loss value) ITM transmission.

#### 4.2.2.5.1 Micro-roughness: prompt loss

On small enough scales  $\lambda_s$  the scatter from an isotropically “super-polished” surface is known to be closely  $\mathcal{L}_S = [4 \pi \sigma(\lambda_s) / \lambda]^2$ , in the “micro” regime  $\sigma(\lambda_s) / \lambda \ll 1$ . Ideally this would define micro-roughness (distortions included in PSD integrated down to a  $\lambda_s$  cutoff where this simple loss formulation breaks down). In order to reduce the requirement for all short  $\lambda_s$  (cutoff  $\sim 2\text{mm}$ )

imperfections to a single rms value, some reasonable assumptions (appendix H of E950099-04-D) are needed, based on the condition  $\lambda_{s,\text{cutoff}} \ll 2w$ . When defined this way, the micro-roughness merely parameterizes prompt diffuse scatter loss, which, at 1064 nm, is  $\sim 5$  ppm/surface for isotropic polished surface micro-roughness = 0.2nm rms (appendix H of E950099-04-D). It has been demonstrated (OTF TIS scatter scan of MCCM4K01) that cavities comprised of such super-polished surfaces coated with the same process to be used for Adv LIGO can have  $\mathcal{L}_S$  at this level (under the condition that cavity  $w_{\text{TM}}$  is sufficiently small to avoid any point defects, see next section).

#### 4.2.2.5.2 Point defect prompt loss

In situ measurements of the LIGO I performance have indicated a much larger prompt loss, tentatively traced to large numbers of defect scatter points embedded in the multi-layer coatings (with potentially significant additional contributions from surface cleaning abrasion and contamination). This anomalous prompt loss can amount to at least  $\mathcal{L}_S \sim 30$  ppm per HR surface. On the other hand laboratory (LIGO OTF) measurements have demonstrated that large area ( $> \text{cm}^2$ ) HR surfaces with mean point scatter contribution of  $< 5$  ppm are available. In fabrication we assume that this defect class can be reliably controlled to  $< 5$  ppm/surface. This, combined with the super-polish micro-roughness scatter limit of  $< 5$  ppm (previous section) gives the combined effective scatter loss entry in Table 3.

#### 4.2.2.5.3 Mid-large scale loss

Larger surface scales  $\lambda_s$  not included in 4.2.2.5.1-2 also can contribute to the arm mode circulating loss (“mid-large” scale loss: the remainder of scattering losses). These distortions also obey  $\sigma(\lambda_s)/\lambda \ll 1$  and therefore can be expected contribute scatter loss bounded by  $< [4 \pi \sigma_F / \lambda]^2 \sim 72$  ppm. However the discussion of 4.2.2.4.2 has identified the specification limit of  $\sigma_F < 0.7 \text{nm}$  as substantially contributing to non-loss scatter (arm cavity modal distortion). The requirement entry (36 ppm cavity total) of Table 4 for this class of loss allows for this (substantiated by the FFT modeling described in 4.2.2.4.1). If this balance proves overly optimistic it appears possible to have the TM surface 1 polished to  $\sigma_F < 0.45 \text{nm}$ . Note that for the macroscopic  $\lambda_s$  scales influential here ( $\sim \text{mm-cm}$ ) there is no reason to anticipate any additional degradation via the HR coating process.

### 4.2.2.6 Loss requirements for the Recycling cavities

The loss budget situation for the RCs is qualitatively somewhat different, hence this separate section. The overall round trip “eigen-mode” loss is typically much higher ( $\sim 100$ s ppm) compared to the arm cavities. Its budget is dominated by aperture diffraction losses (e.g. oblique BS) and transmissive and AR (surface 2) losses, unique to these cavities. AR surface loss can comfortably be specified at  $< 100$  ppm/surface. Sufficient FFT modeling has been completed to bound the diffractive loss incurred by the limiting aperture elements (PR3, SR3 and BS) to  $< 200$  ppm (even for mode match to any arm mode allowed by the tolerancing requirements of section 4.2.2.3.7). Figure 3 gives an overview of the impact of net RC loss on the inspiral ranges and PRC gain respectively.

Achieving the 1000 ppm RC loss budget limit (LIGO-T070075-01) requires good matching, and low aberration scattering loss (analogous to section 4.2.2.5.3). Since the optical finish of the RC COC are comparable to those of the arms (see table 4) we anticipate all these “fabrication” sources

of scattering loss to be negligible on the 1000ppm scale. The possible exception has to do with the obliquity of the BS and FM elements where astigmatism can be induced by prism (finite wedge angle) effects and residual sphericity. The design and implementation strategy for the RCs has allowed for adjustment (repositioning of PR2, SR2), and compensation (CP TCS authority) to reduce any mean (i.e. “bull’s eye” mode) miss-match due to optic fabrication tolerances (table 5); thermal effects; and setup errors (described in LIGO-T080198-00).

Even with such compensation of mean spherical distortion due to BS wedge or BS/FM non-flatness, the induced astigmatism of these distortions remains. Consideration of the BS wedge astigmatism motivated re-configuration of the COC allowing a small BS wedge ( $0.04^\circ$ , table 2). This causes an astigmatic wavefront distortion ( $\pm$  sag over the beam Gaussian diameter) of  $< 1\text{nm}$  ( $\pm$ 2000 km ROC). This level of modal distortion loss is entirely negligible. On the other hand the astigmatic wave-front distortion due to reflection (at  $45^\circ$ ) from a spherical surface of ROC  $R_X$  would be  $R_X/rt[2]$ . The mismatch effect of a lens of this amplitude has been studied in T080198-00, and T0900384-v1. The worst case of such mismatch would contribute an additional equivalent RC loss of  $\sim 2000\text{ppm}/G_{RC}$  for  $R_X \sim 200\text{km}$ , which is within the net loss budget and sets the flatness requirement in table 2.

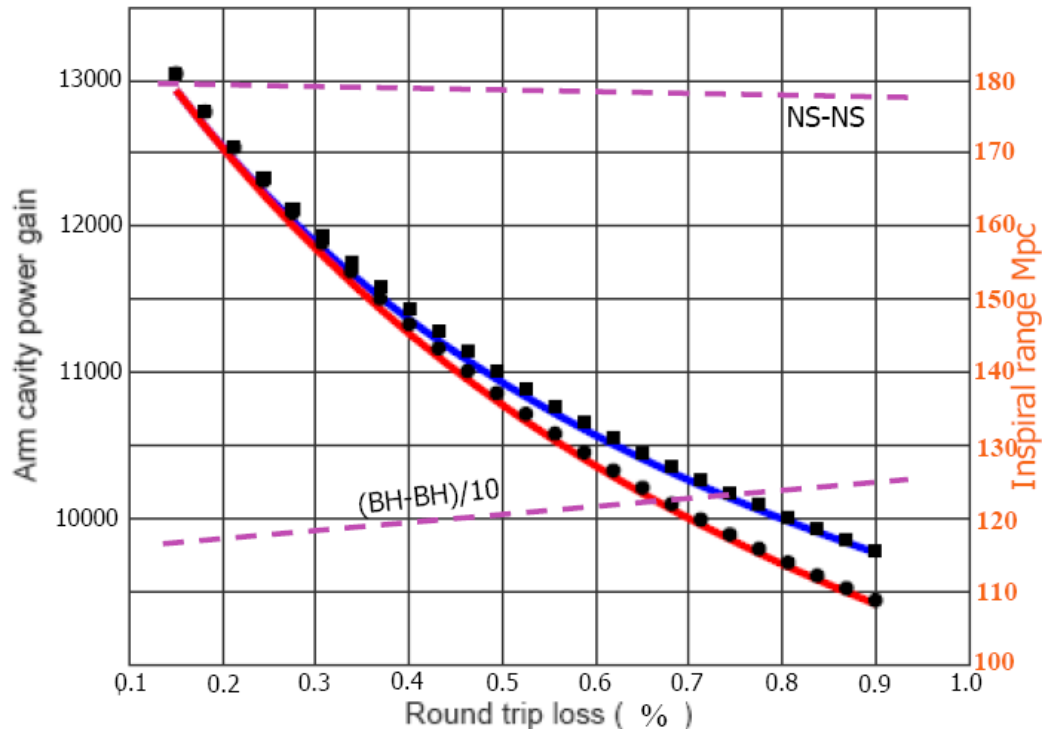
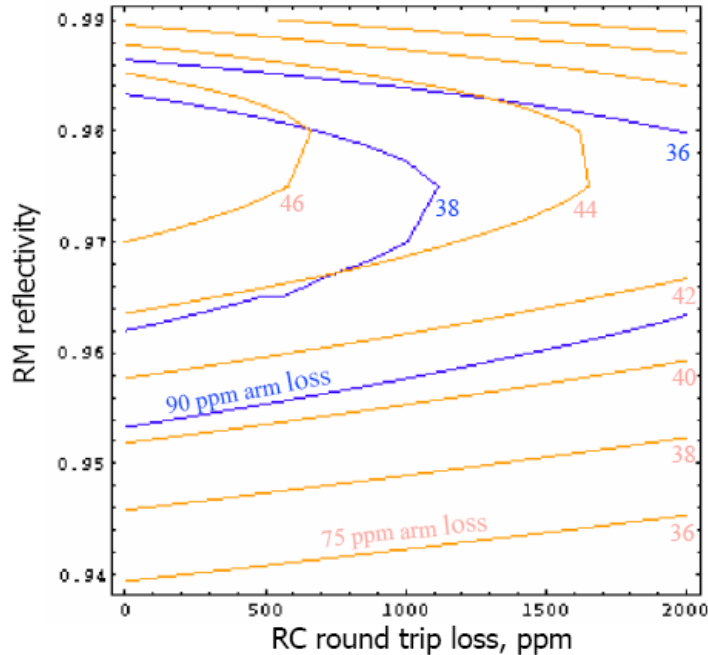


Figure 3. Upper plot illustrates influence of RC loss on inspiral ranges. Note the qualitative similarities to Fig. 2 (all curves have same definition as in Fig. 2). Calculated from Bench62 with phase and RM reflectivity optimizations.



Contours of constant  $G_{RC}$  families for 75 ppm  $L_A$  (orange) and 90 ppm  $L_A$  (blue). The high values of  $G_{RC}$  included pertain to the PRC

#### 4.2.2.7 Absorption: losses and thermal effects

Absorption, as in LIGO I, is anticipated (based on the known quality of LIGO I coatings) to be a minor contributor to the net loss budget. However its indirect effect via thermal distortion scatter loss from the  $TEM_{00}$  mode must be stringently limited for the much higher beam power design of advanced LIGO. These full power thermal distortions would significantly deteriorate (R. Lawrence, MIT thesis, 2003) the carrier fields (not just side bands as in LIGO I). Concern that the absorption may not be sufficiently uniform, as well as mixed success with the “point design” compensation polish (of the RM) approach in LIGO I lead to the entirely new design here of active compensation with auxiliary correction plates (LIGO-T060083-01-D) and TM ring heaters.

In addition, the total (bulk plus surface) absorption of beam power will significantly raise the TM mean temperature. The absorption goal values described below will raise their temperature  $\sim 11^\circ$  K above [radiative] ambient (includes beam heating and TCS compensations). Approximately 3 times this absorption goal (e.g. from an accumulation of 1ppm mean contamination absorption) will result in a net compensated TM temperature rise of  $\sim 21^\circ$  K ( $4.5^\circ$  K from beam heat, and  $16^\circ$  K from compensation. See LIGO-T060214-01). This alone will increase the thermodynamic noise contribution in the signal channel by  $\sim 3\%$ .

**Table 5 Specified limits to losses (in ppm) in COC optics**

Section reference	Loss Source	Input TM	End TM	BS Mirrors	Fold Mirror	Recycling Mirror
4.2.2.7.3	Bulk scattering of transmitted beams	<50	N/A	< 50	N/A	< 50
4.2.2.7.2	Total surface absorption Surface 1	< .5*	< .5*	<1	<1	< 1
4.2.2.5.1,2	Surface scattering from effective mirror roughness, defects Surface 1	<10*	<10*	<100	<50	<200
4.2.2.7.4	Ghost beam loss (surface 2 origin)	<50	N/A	<50	N/A	<1000
4.2.2.7.5.1,2	Cumulative contamination scattering Surf. 1	< 4*	< 4*	<20	<10	<10
4.2.2.7.2,5	Cumulative absorption Surface 1	<1*	<1*	<4	<4	
0	Substrate bulk absorption, single pass	< 40	N/A	<2	N/A	<60
4.2.2.3.4	ETM transmission	N/A	<6	N/A	N/A	N/A
4.2.2.4.6	Finite COC apertures, $\phi_e$ diffraction loss	0.4*	2*	20	10	N/A
4.2.2.5.3	Mid-Large scale surface scattering losses		<36*		<50	
	cavity mode RT total loss		<80* Arm	<1000 Recycling		

\*The green highlighted quantities are anticipated specific source losses. Their sum (last row) constitutes a target net loss budget requirement.

#### 4.2.2.7.1 Bulk absorption

Although thermal distortion through the COC substrates is required to be correctable by an AOS subsystem (CP compensation), it is clear that low average substrate absorption will be crucial to make the entire design work. In this spirit we require the ITMs to have mean central ( $\phi = 2w$ ) absorption of  $\leq 2 \text{ ppm/cm}$ . Special low OH content FS will probably be required to meet this, in particular to assure that non-uniform absorption will not cause significant wave front distortion. For the case of the BS element, we anticipate holding the magnitude of lensing and thermal strain (it having more severe problems having to do with beam heating due to its thinness and  $45^\circ$  incidence) to manageable levels by requiring ultra low absorption,  $<0.2 \text{ ppm/cm}$ , material (Heraeus 3000 series).

#### 4.2.2.7.2 Surface absorption

Unlike initial LIGO, the arm power levels in advanced LIGO cause a significant [HR coating] absorption thermal distortion of the arm cavity mode. To control this (at the  $R_{\text{eff}}$  operating point of figure 1) TCS ring heaters are necessary for compensation. Current design of these heaters imposes a coating absorption limit of 0.9 W/surface, requiring coating absorption  $< 1 \text{ ppm}$  (at arm beam power= 0.85 MW). For COC fabrication we will nominally require coating absorption  $<0.5 \text{ ppm}$  (achieved so far in samples) with a best effort to achieve  $<0.3 \text{ ppm}$ . The successful TCS regulation

of iLIGO (20W beam power) is consistent with TCS/AOS design of advanced LIGO based on these absorption requirements.

#### 4.2.2.7.3 Bulk scattering

It is assumed that this category of loss does not contribute to substrate heating. The requirement value is chosen to make this contribution to loss much smaller than that from other mechanisms. Expected scattering loss from high homogeneity FS is much less ( $< 2\text{ppm/cm}$ ).

#### 4.2.2.7.4 Ghost beams

Here the transmission residual beam through the HR-ETM is not included (see 4.2.2.3.4). Then all other ghost reflections are recycling cavity losses. Single ghost losses  $>200$  ppm become significant with respect to the net RC loss budget. The table 4 values are required to keep this balance. AR coatings can feasibly limit reflection to  $< 50$  ppm, sufficient for all dumped ghost beams. In one instance (the BS) an AR surface acts to relay a picked off interferometer field sample. Exact specification for this reflectivity to assure adequate signal for low power operation is TBD. Significantly lower AR reflectivity implies very close cancellation of layers, which may be highly susceptible to thermal noise or other instabilities. For beams transiting the AR coatings a full analysis shows that there is no similar sensitivity to coating uniformity variation.

#### 4.2.2.7.5 Contamination loss

This requirement derives from 4.2.2.7.2: any acquired surface absorptive loss should be substantially less than the requirement there. It is assumed that this extremely stringent limitation will keep any concomitant scatter loss negligible. A time scale needs to be attached to such accumulation. See LIGO-E990035-C, subsequently updated in LIGO-E070304-00.

### 4.2.3 Interface Definitions

The main interface for COC occurs with the suspension subsystem. The COC subsystem includes the substrate and all coatings that are applied to it. There are only mechanical and optical interfaces to the COC.

#### 4.2.3.1 Interfaces to other LIGO detector subsystems

##### 4.2.3.1.1 Mechanical Interfaces

Mechanical interfaces SUS-COC are:

- Location and surface quality of the flat polished onto the edge of each TM optic. This flat is used for attaching the suspension mechanism. From SUS
- Location of alignment reference marks must be well located in order to guarantee proper placement of the optic within the suspension. From SUS
- Mass tolerance and therefore dimensional tolerances must be negotiated with SUS.

Mechanical interfaces SUS-COC-AOS are:

- Size of thermal compensation plates. From SUS and AOS.

#### 4.2.3.1.2 Optical Interfaces

Optical interfaces SUS-COC-IO are:

Optical interfaces COC-ISC are:

- Diagnostic beams which interface to the ISC subsystem and are either input to COC from the ISC or derivative from the primary IFO beams (e.g. ghost beams off wedged AR surfaces). Each COC must have some minimum wedge to keep second surface reflections out of the main beam path. The requirement for pointing the ghost and diagnostic beams determines the wedge angles of the COC.
- AR coatings may be designed to reflect ASC positioning beams. ASC requirements shall not compromise the performance of the COC.

Optical interfaces COC-AOS are:

- Optical absorption of thermal compensation plates. Coatings, material quality and surface quality of thermal compensation plates will be determined by COC and will be in accordance with the loss budget for the recycling cavity.
- The absorption profile of compensation plates and ITMs will be measured by COC and reported to AOS.

#### 4.2.3.1.3 Stay Clear Zones

To maintain the good optical performance required of the COC optical faces it will be necessary to maintain a stay clear cone whose vertex is on the optical axis and whose surface intersects the  $\sim 1$ ppm contour of the Gaussian beam intensity at any mirror face. This prescription is to include a  $\sim 5$ mm margin for imperfect alignment and suspension settling. Intrusion within these [cylindrically symmetric] cones can be tolerated as long as the intruders for one face “clip” geometrically no more than  $\sim 1$ ppm of the impinging beam intensity.

#### 4.2.3.2 Interfaces external to LIGO detector subsystems

There are no interfaces to COC aside from those to other LIGO subsystems.

#### 4.2.4 Reliability

- It is expected that the COC have no inherent hard failure mechanisms. Reliability will be essentially dependent on the extent that they remain free of contamination from external sources. As long as any contamination is removable (via cleaning, which has been our experience in LIGO to date) then we define this as not being a [permanent] failure. It is possible that contamination, either included during fabrication or acquired during installation/operation, could permanently “burn” onto COC surfaces causing failure (needing replacement). In the former case these should be rejected by our acceptance testing requirements/program. The former case would be true failure (no such examples yet seen) addressed by our requirement for COC spares (see COC design, E080494-v2).

- An adequate protocol for handling, storing, cleaning, and working around the COC elements must be formulated and assured in practice to avoid breakage or degradation of the optical surfaces. It is to be noted that a single inadvertent scratch on a coated surface will likely constitute breakage.
- The COC shall design handling fixtures, storage & shipping containers and procedures to assure low risk of failure during standard processing steps such as cleaning, inspection and phase map metrology.

#### 4.2.5 Maintainability

It will not be possible to “repair” COC elements. The only form of maintenance will be in cleaning the optical surfaces. There is no inherent contamination mode so that a mean time to repair for cleaning will not be a requirement imposed on the COC.

- It will be required that effective cleaning procedures for the specific COC materials (fused silica and the optical thin film coating materials) be developed which can be invoked to clean the surfaces when they are determined to be contaminated.
- Tests (e.g. in-situ ring down, scattered light monitors, ellipsometry, etc.) must be developed to unambiguously signal contamination since in-situ cleaning or change out of COC elements will cause major LIGO down time.
- Given the COC operational environment (UHV) it is anticipated necessitating removal for the purpose of cleaning is impractical on a routine operational basis. Therefore every effort will be made to investigate and develop in-situ cleaning procedures.
- Consistent with the on time requirements of advanced LIGO IFOs at their nominal strain sensitivity, is that contamination equivalent to that in Table 4 not accrue in less than 1 year’s operating time. This estimate is based on the assumption that replacing or cleaning the contaminated mirrors will cost an effective observation down time of one month.

#### 4.2.6 Environmental Conditions

COC elements must be exposed at all times to only the cleanest possible environments.

For storage and transport, individual, specially designed hermetic containers will be provided which assure an environment of at least a Class10 clean room environment. Except for testing and measurement that need direct access to the COC bare optical surfaces, and for as long as practically feasible through final installation in their respective IFO vacuum chambers, COC optics are to have their contamination sensitive face surfaces protectively sealed with First Contact™ film (per LIGO-E1000079).

For open handling, transfer to the IFO chambers, cleaning, and auxiliary examination or testing the elements will be exposed to no worse than a Class 100 clean room environment.

The cleanliness requirement for the COC is particularly critical, since first, contamination can lead to *cumulative* irreversible degradation of the optical performance and hence extremely small

detectable amount is of concern. Second, cleanliness of the entire LIGO vacuum environment is specified by its impact on the COC, so that all other subsystems are in turn specified in this respect by the COC requirements. Cleaning of COC in preparation for installation is specified in LIGO-E990035-C subsequently updated in LIGO-E070304-00.

#### 4.2.6.1 Natural Environment

##### 4.2.6.1.1 Temperature and Humidity

**Table 6 Environmental Performance Characteristics**

Operating	Non-operating (storage)	Transport
+0 C to +50 C, 0–90 % RH	-40° C to +70 C, 0–90 % RH @ <10° C/Hr.	-40° C to +70 C, 0–90 % RH @ <10° C/Hr.

##### 4.2.6.1.2 Atmospheric Pressure

##### 4.2.6.1.3 Seismic Disturbance

#### 4.2.6.2 Induced Environment

Only approved materials shall be put in close proximity of the optical surfaces for extended periods of time (even short term placement is to be checked with cognizant optical engineer)

##### 4.2.6.2.1 Electromagnetic Radiation

All COC Coatings are extremely sensitive to UV radiation. Severe, non-reversible damage to the coatings can occur with even short term exposure to UV sources. UV sources include direct exposure to welding flash, UV curing lamps, high UV output lamps, UV lasers/markers, plasma discharges, intense direct sunlight, etc. Consult the appropriate optical engineering staff before a potential exposure.

##### 4.2.6.2.2 Acoustic

##### 4.2.6.2.3 Mechanical Vibration

#### 4.2.7 Transportability

All items shall be transportable by commercial carrier without degradation in performance. As necessary, provisions shall be made for measuring and controlling environmental conditions (temperature and accelerations) during transport and handling. Special shipping containers, shipping and handling mechanical restraints, and shock isolation shall be utilized to prevent damage, as specified in LIGO-E070070-00 and LIGO-T070293-00). All containers shall be movable for forklift. All items over 100 lbs. which must be moved into place within LIGO buildings shall have appropriate lifting eyes and mechanical strength to be lifted by cranes.

### 4.3 Design and Construction

Minimum or essential requirements that are not controlled by performance characteristics, interfaces, or referenced documents. This can include design standards, requirements governing the use or selection of materials, parts and processes, interchangeability requirements, safety requirements, etc.

#### 4.3.1 Materials and Processes

All design drawings shall be in accordance with the Drawing Requirements, [E030350-A](#).

##### 4.3.1.1 Finishes

See section 4.2 for requirements regarding surface polish and coatings.

Standard <40-20 polishing quality on all not otherwise specified COC surfaces. All Coatings optical coatings applied to COC surfaces to be individually specified hard, low loss, ion beam sputtered.

##### 4.3.1.2 Materials

See section 4.2 for fused silica material callout for the optics.

All tooling which contacts the optics must be compatible with the Class B specification of the LIGO Contamination Control Plan, [M990034-C](#).

##### 4.3.1.3 Processes

###### 4.3.1.3.1 Welding (not applicable)

###### 4.3.1.3.2 Cleaning

The COC must be cleaned either with First Contact™ per [E070292-00](#), or with Liquinox and DI water per LIGO-E990035 (subsequently updated in LIGO-E070304-00)

##### 4.3.1.4 Component Naming

All components shall be identified using the LIGO Naming Convention (LIGO-E950111-A-E). This shall include identification (part or drawing number, revision number, serial number) physically stamped on all components, in all drawings and in all related documentation. The convention for these names and markings is specified in the advanced LIGO PDD (LIGO-T080033).

**4.3.2 Workmanship (not applicable)****4.3.3 Interchangeability (not applicable)****4.3.4 Safety**

This item shall meet all applicable NSF and other Federal safety regulations, plus those applicable State, Local and LIGO safety requirements. A hazard/risk analysis shall be conducted in accordance with guidelines set forth in the LIGO Project System Safety Plan LIGO-M950046-D, section 3.3.2. (and in accord with updates in LIGO-M960001-Final4). All items described here shall be in compliance with Adv. LIGO safety procedures as outlined in LIGO-M070360).

**4.3.5 Human Engineering (not applicable)**